Thermo-poro-mechanical modeling of RTV intumescence

Sreevishnu Oruganti[1,2], Sergio Fraile Izquierdo[3], Nagi N. Mansour[3] and Francesco Panerai[1,2]

[1] Department of Aerospace Engineering, University of Illinois Urbana-Champaign, IL-61801, USA

[2] Center for Hypersonics and Entry System Studies, University of Illinois Urbana-Champaign, IL-61801, USA

[3] Analytical Mechanical Associates Inc. Moffett Field, CA-94035, USA

September 2nd, 2026

This work is supported by a NASA Space Technology Graduate Research Opportunities Award, grant number 80NSSCC22K1192.

Introduction

- To protect spacecraft from extreme heat during atmospheric entry, a Thermal Protection System (TPS) is required:
  - For high-speed entries, ablative heatshields such as Phenolic Impregnated Carbon Ablator (PICA) or Avcoat are used,
  - Large heatshields are tiled and are bonded with a silicone elastomer gap-filler, known as RTV560.

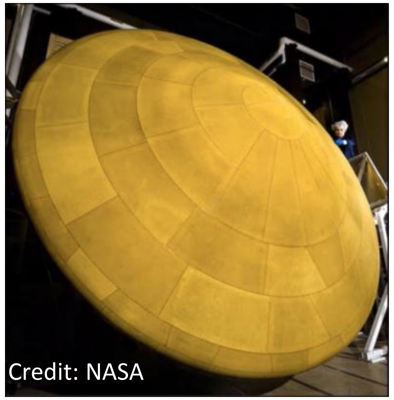

Mars Science Laboratory (MSL) heatshield with tiled PICA bonded by RTV560, *Beck 2014*[2].

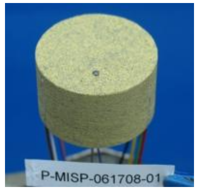

Instrumentation plug on the MSL heatshield, *Beck 2014*[2].

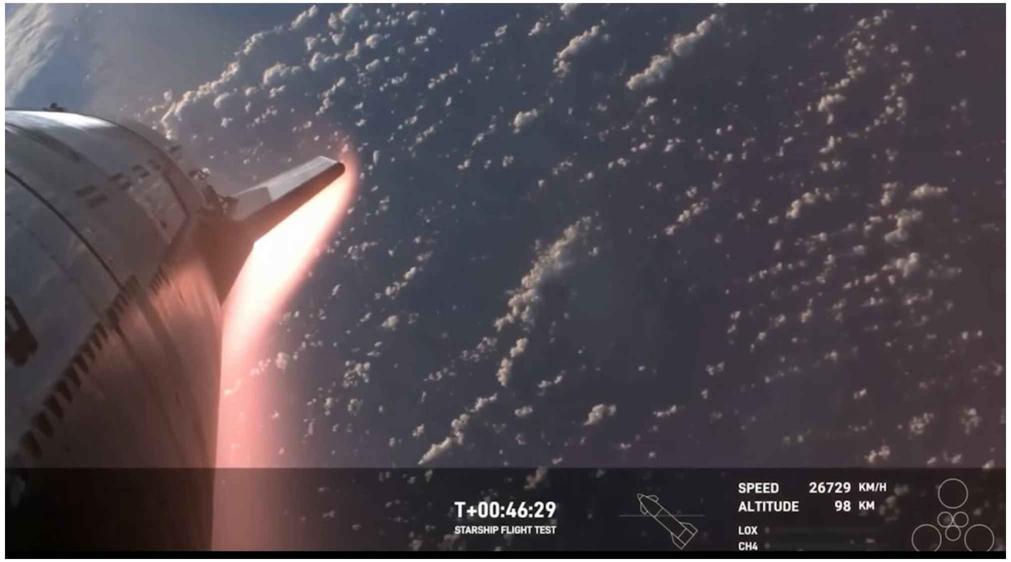

SpaceX Starship atmospheric (re)-entry. [Credits: SpaceX]

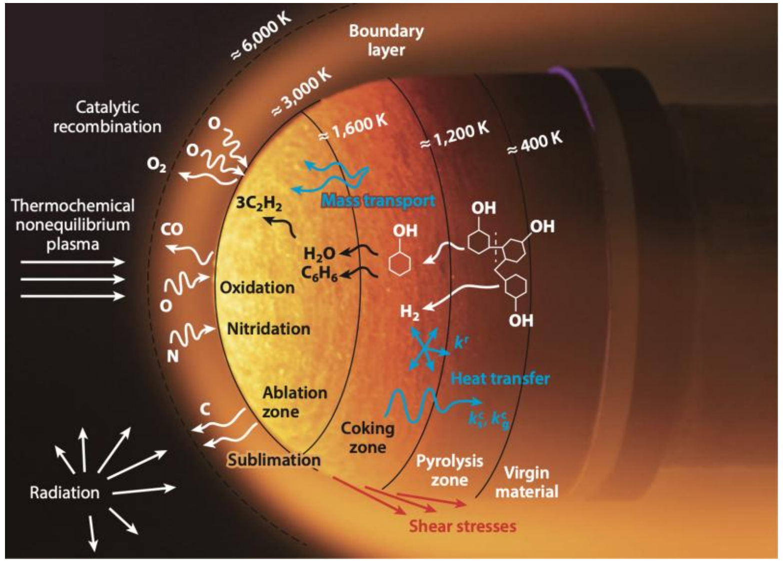

Illustration of the ablation phenomenon, *Mansour 2024*[1].

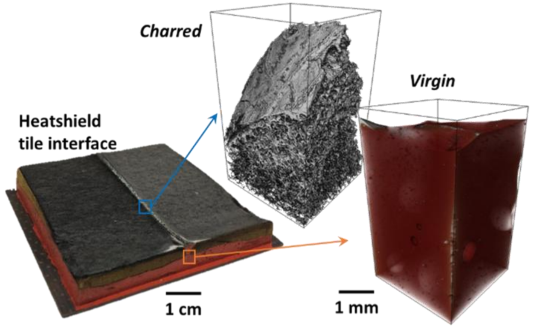

Tiled heatshield showing virgin and charred RTV, *Oruganti 2023*[3].

RTV Intumescence

- Numerous tests (flight and ground) have shown adverse effects of RTV as a gap-filler as it:
  - Swells (or intumesces) as it's heated, and can transition flow to turbulence,
  - Melts over heatshield and contaminates sensors, changing surface properties,
  - Current material response models do not account for these effects of RTV.
  - **Goal of my PhD was to study and model decomposition, swelling and ablation of RTV.**

Post-flight heat shields for SpaceX Dragon and Varda W2 capsules.

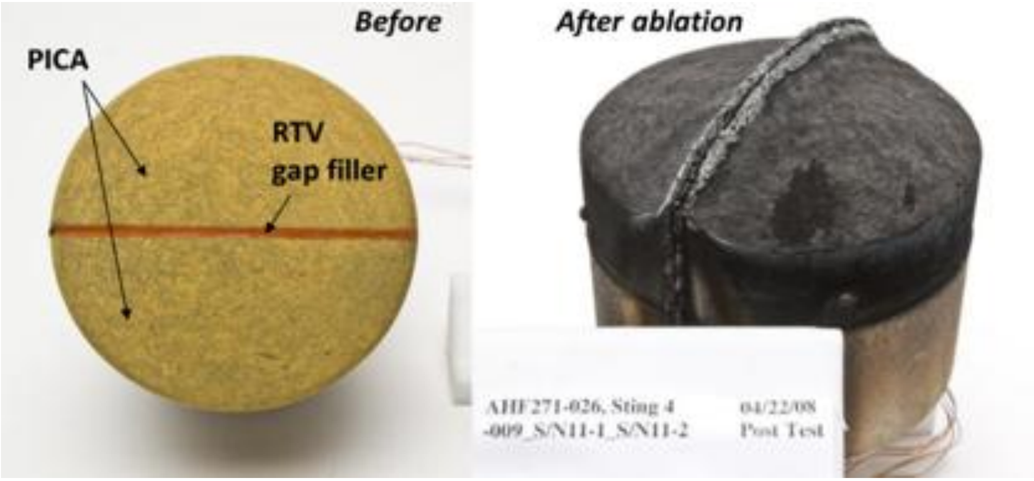

RTV fencing in PICA, Beck 2014[2].

Experimental Characterization

Pyrolysis mechanism

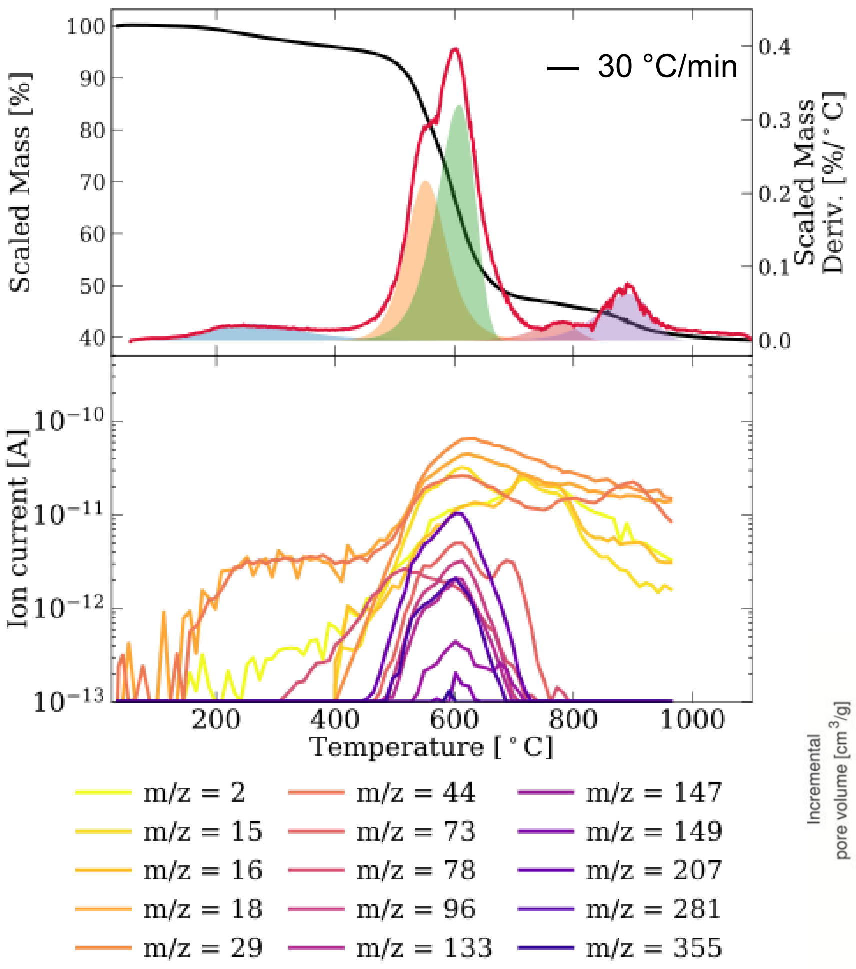

TGA-MS of RTV at 30 °C/min

Virgin vs char characterization

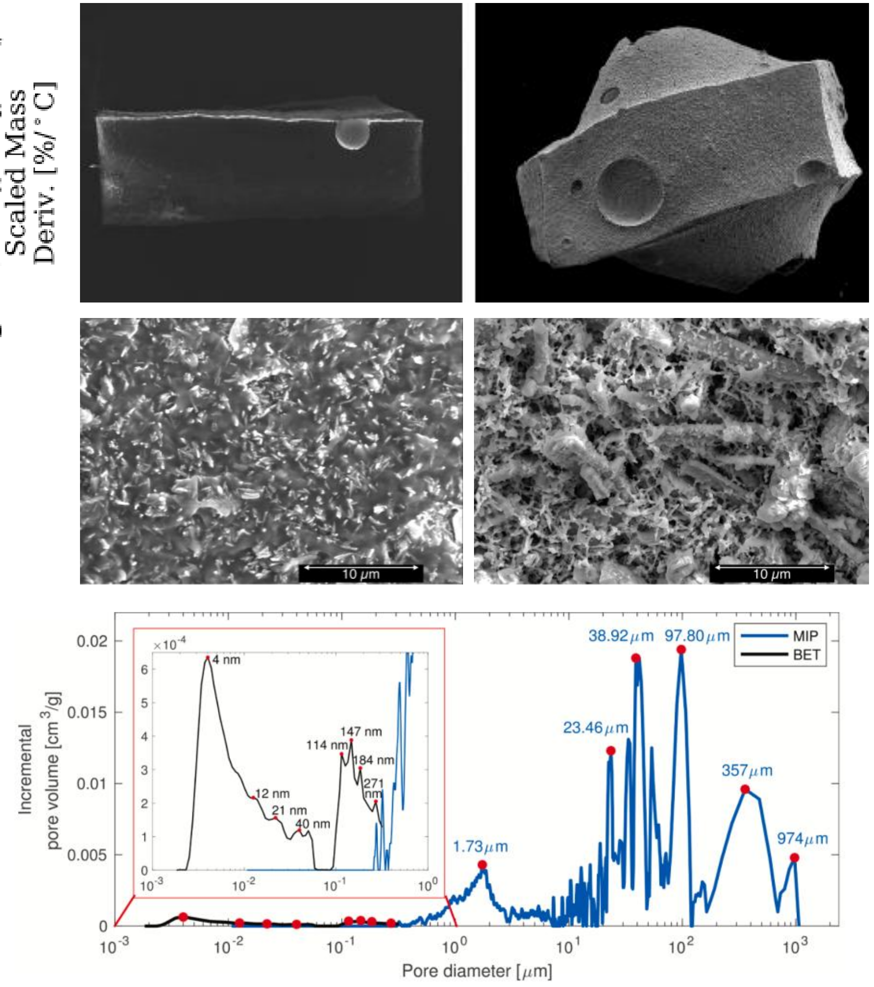

Electron microscopy and porosimetry of charred RTV

In situ Micro-CT at the Advanced Light Source

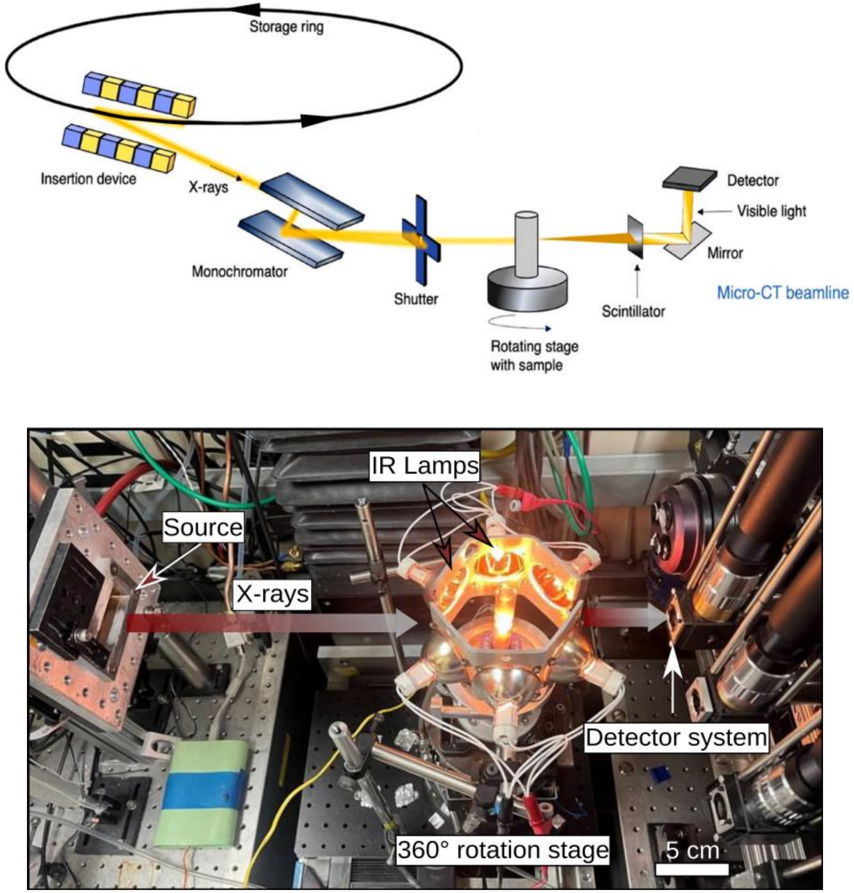

Schematic of ALS and layout of in situ micro-CT setup

In situ Micro-CT of RTV

64 °C/min

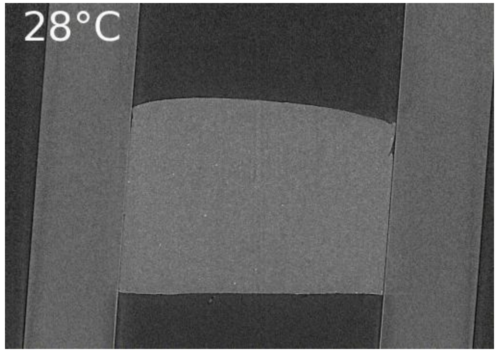

228 °C/min

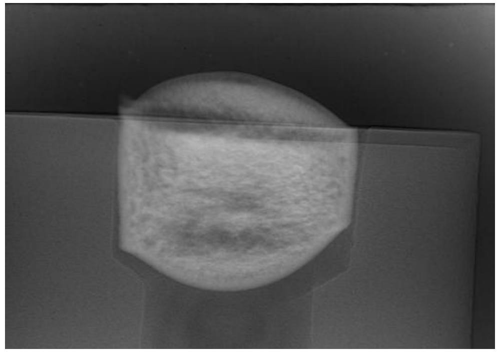

1946 °C/min

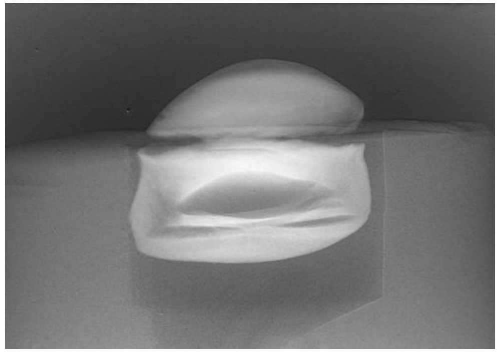

N_2 plasma test at Plasmatron X

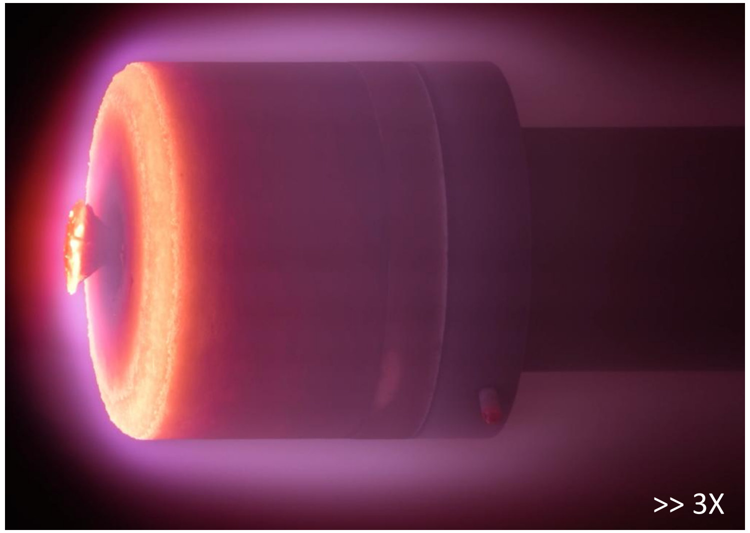

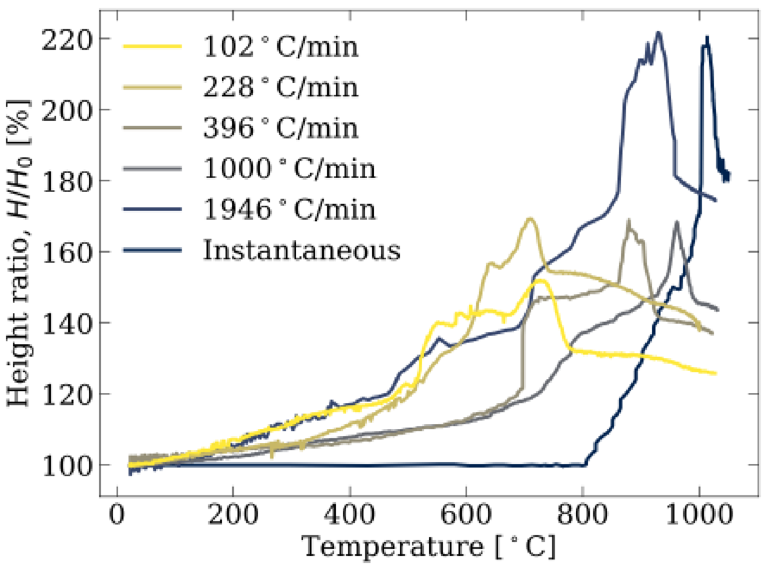

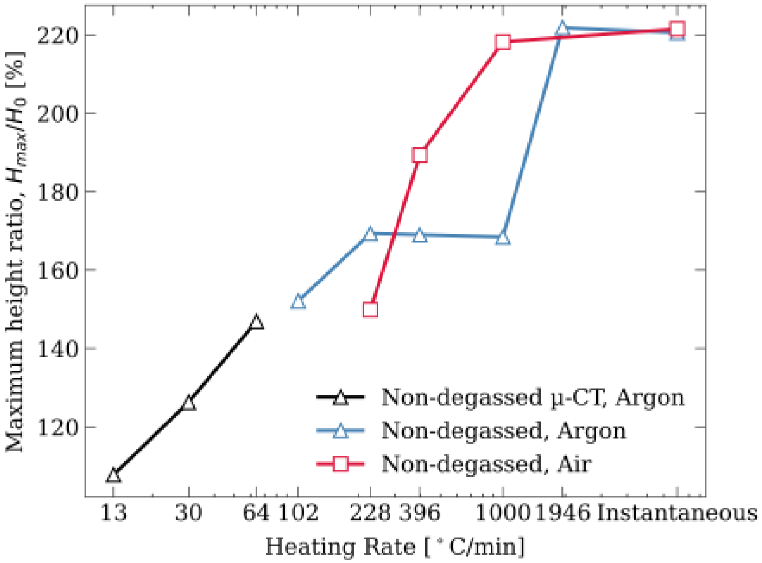

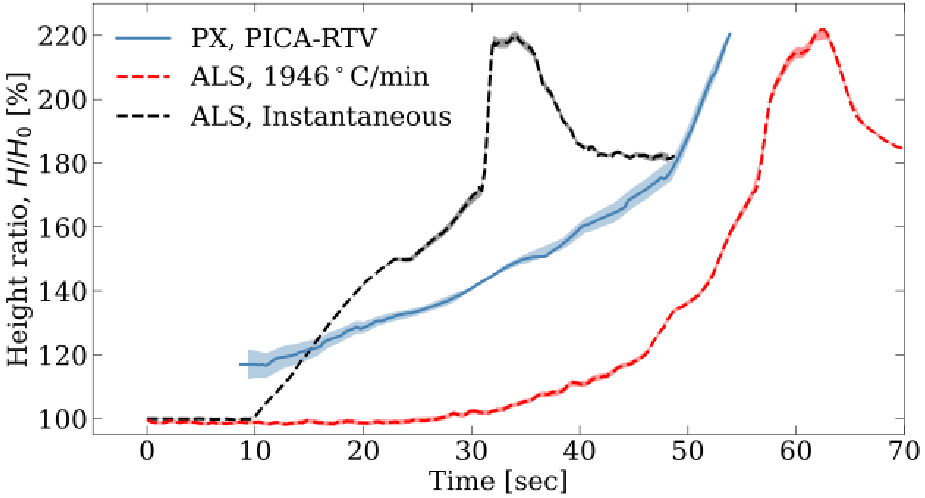

Intumescence mechanism

- RTV has closed pores filled with trapped gases and adsorbed water,
- Heating causes swelling due to pressure build up within the closed pores, which occurs until
  - Adequate pressure is developed in the pores to form a crack and outgas, or
  - Adequate time is given for the RTV to pyrolyze and form a porous network to outgas.
- Goal is to develop a model in PATO:
  - PATO is a finite-volume code that assumes volume-averaging,
  - Is coupled with solid mechanics to simulate volume change due to swelling or shrinking,
  - Current model doesn't consider cracking and surface chemistry for simplicity.

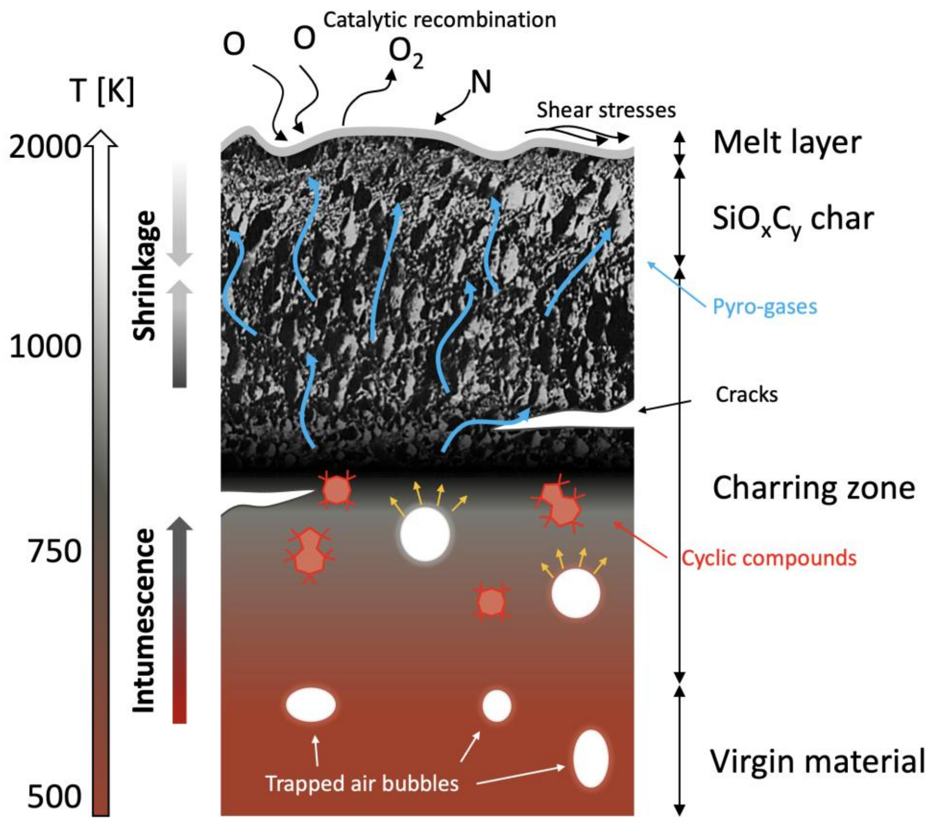

Introduction of closed porosity in PATO

- Volume-averaging within REV:
  - Each phase is composed of several sub-phases that decompose into open porosity,

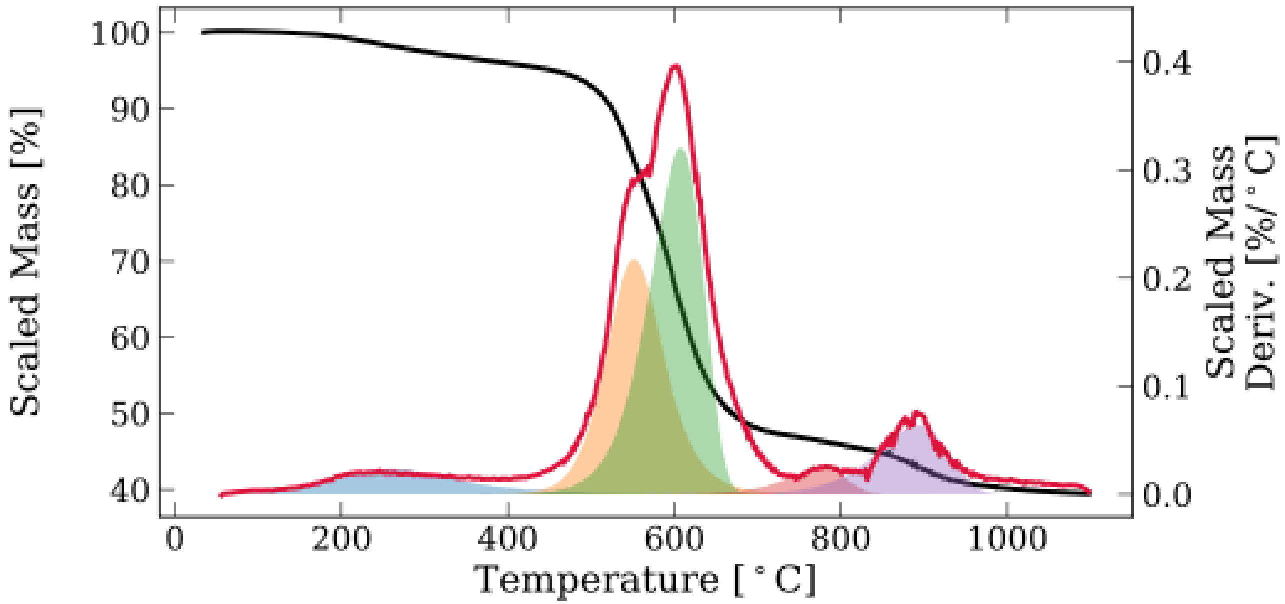

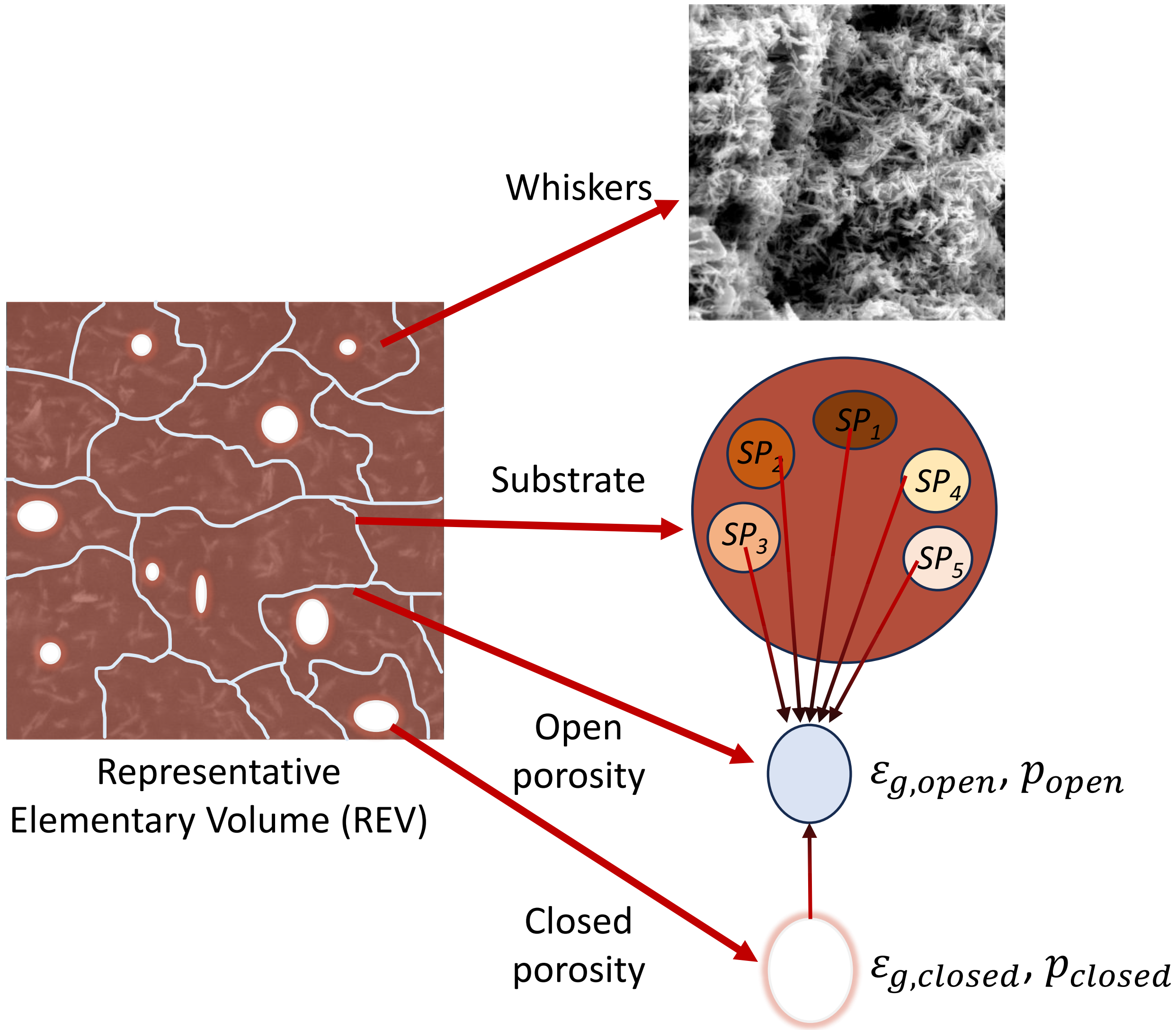

Introduction of closed porosity in PATO

- Volume-averaging within REV:
  - Each phase is composed of several sub-phases that decompose into open porosity,
  - Closed porosity is not considered in PATO.
- New model for closed porosity developed as $p_{open} \neq p_{closed}$,
  - p_{open} derived using mass and momentum transport (Darcy Law),
  - p_{closed} obtained using ideal gas law.
- Effective volume-averaged pressure
  - $p_{eff} = \frac{(\varepsilon_{g,open}\, p_{open} + \varepsilon_{g,closed},\, p_{closed})}{(\varepsilon_{g,open} + \varepsilon_{g,closed})}$

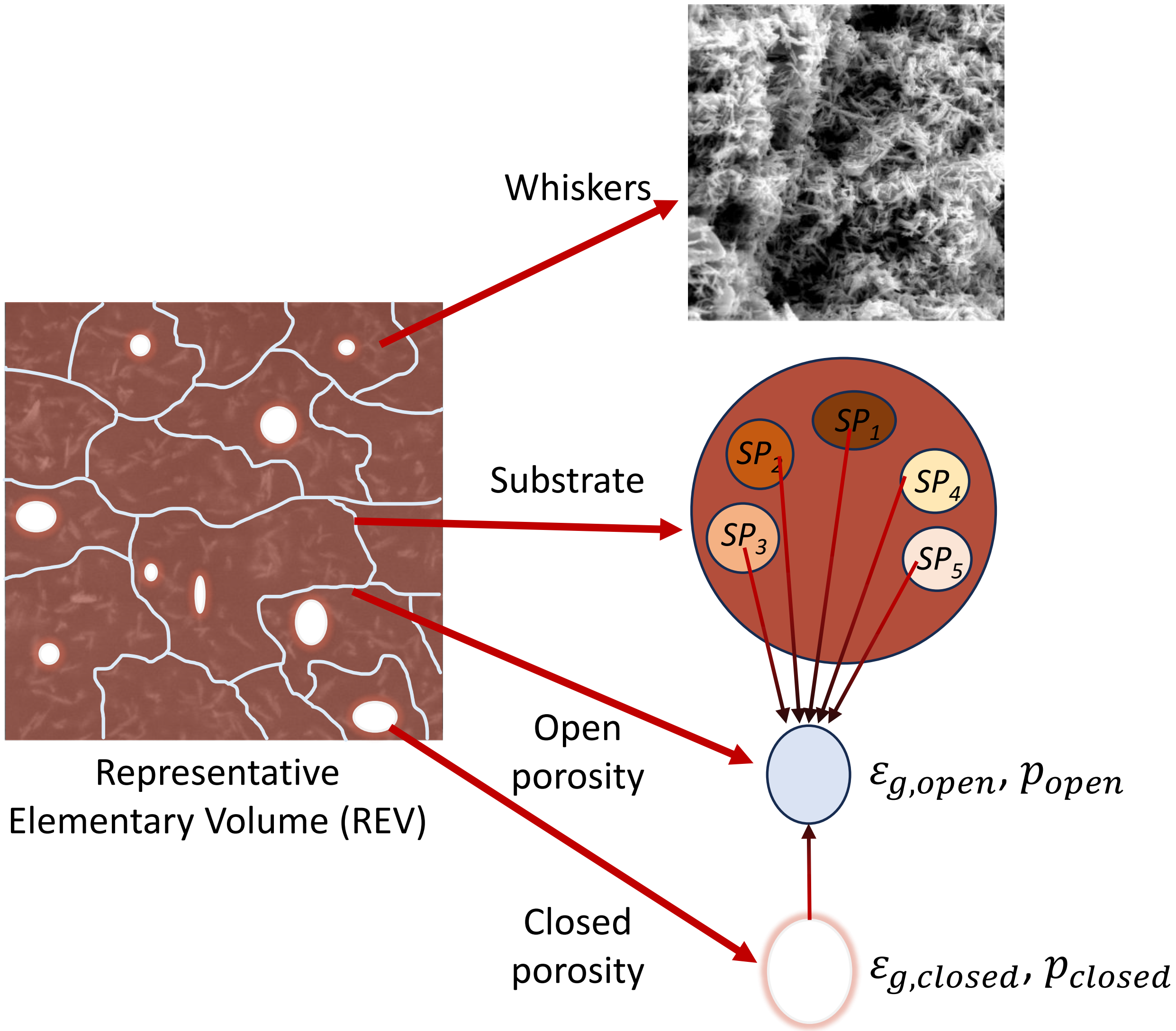

Thermo-poro-mechanics

- Deformation of RTV occurs due to thermal expansion, pressure build-up and pyrolysis shrinkage
  - Assuming isotropic linear elastic material, incremental deformation is modeled as:

$$\frac{\partial}{\partial t}\left(\rho\frac{\partial \boldsymbol{D}}{\partial t}\right) = \nabla\cdot((2\mu+3\lambda)\nabla\boldsymbol{D}) + \nabla\cdot\left[\underline{\sigma_s} - \frac{\Delta p_{eff}}{\varepsilon_{g,o}+\varepsilon_{g,cl}}(\varepsilon_{g,cl})\underline{\mathbf{I}} - (2\mu+3\lambda)\nabla\boldsymbol{D}\right] - \nabla(\Delta p_{eff})$$

  - Key terms:
    - Incremental strain: $\underline{\epsilon} = \underline{\epsilon_s} + \underline{\epsilon_T} + \underline{\epsilon_\xi} = \frac{1}{2}\left(\nabla\boldsymbol{D} + (\nabla\boldsymbol{D})^T\right)$
    - Strain due to applied stresses: $\underline{\epsilon_s} = \frac{1}{2\mu_s}\underline{\sigma_s} - \frac{\lambda}{2\mu(3\lambda+2\mu)}\mathbf{Tr}(\underline{\sigma_s})\underline{\mathbf{I}}$
    - Thermal expansion: $\underline{\epsilon_T} = \alpha(\Delta T)\underline{\mathbf{I}}$
    - Pyrolysis strain: $\underline{\epsilon_\xi} = \frac{V^f - V^0}{V^0}(\Delta\xi)\underline{\mathbf{I}}$

Multi-pyrolysis material-variation model

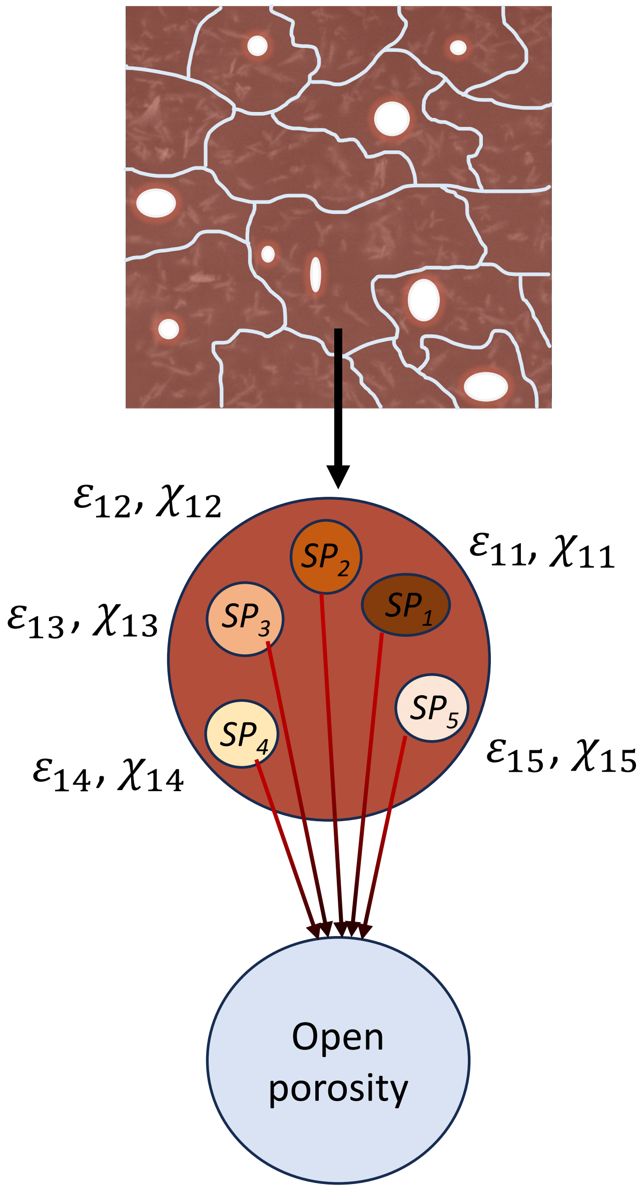

Advancement of pyrolysis of each sub-phase:

$$\frac{\partial \chi_{ij}}{\partial t} = T^{n_{ij}} \mathcal{A}_{ij} exp\left(\frac{-\mathcal{E}_{ij}}{RT}\right)(1-\chi_{ij})^{m_{ij}}$$

Total pyrolysis advancement:

$$\tau = \sum_{i}^{N_p} \sum_{j}^{N_{sp}} \frac{\varepsilon_i^0 \rho_i^0 \mathcal{F}_{ij}}{\sum_i^{N_p} \sum_j^{N_{sp}} \varepsilon_i^0 \rho_i^0 \mathcal{F}_{ij}} (1-\chi_{ij})$$

Material property variation based on overall virgin/char properties

$$\mathcal{Q}(\tau) = \mathcal{Q}_c + (\mathcal{Q}_v - \mathcal{Q}_c)\tau$$

Assumes monotonic variation of material properties with temperature and τ!

Volume-fraction variation of each sub-phase:

$$\frac{\partial \varepsilon_{ij}}{\partial t} = -\varepsilon_{ij}^0 \frac{\partial \chi_{ij}}{\partial t}$$

Material property variation using sub-phase virgin/char properties

$$\mathcal{Q}_{ij} = \mathcal{Q}_{ij,c} + \left(\mathcal{Q}_{ij,v} - \mathcal{Q}_{ij,c}\right)\frac{\varepsilon_{ij}}{\varepsilon_{ij}^0}$$

Overall material property variation

$$\mathcal{Q} = \mathcal{Q}_c \frac{\varepsilon_c}{\varepsilon_s} + \sum_{j=0}^{N_{sp}} \mathcal{Q}_{ij} \frac{\varepsilon_{ij}}{\varepsilon_s}$$

Accounts for non-monotonic variations!

RTV Material Properties

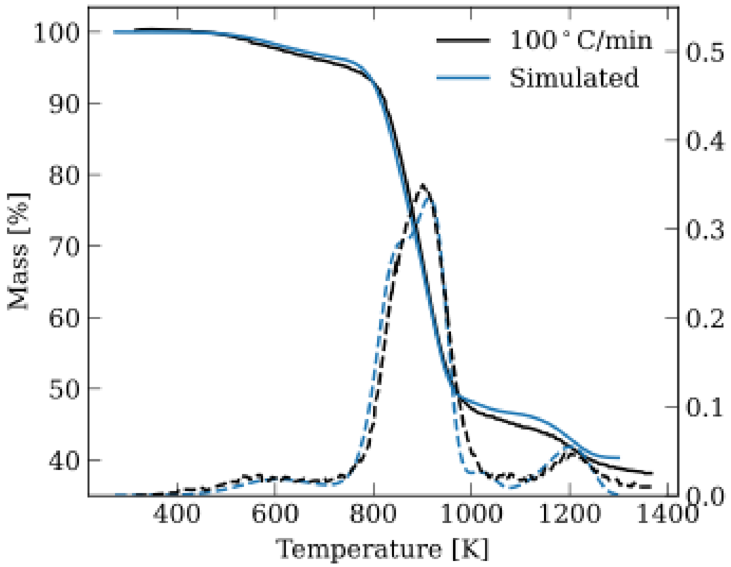

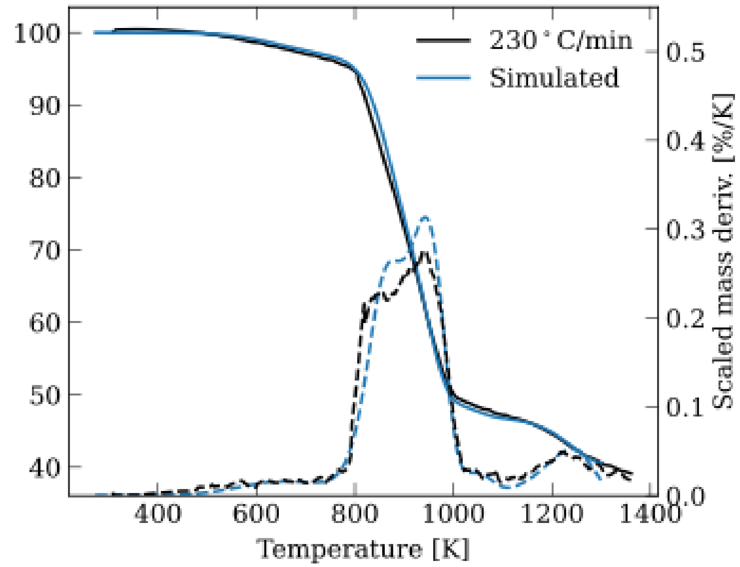

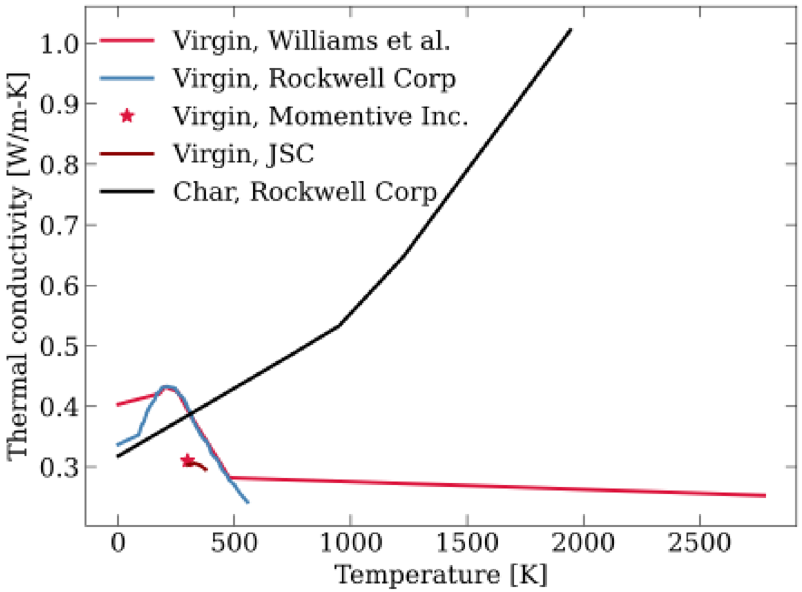

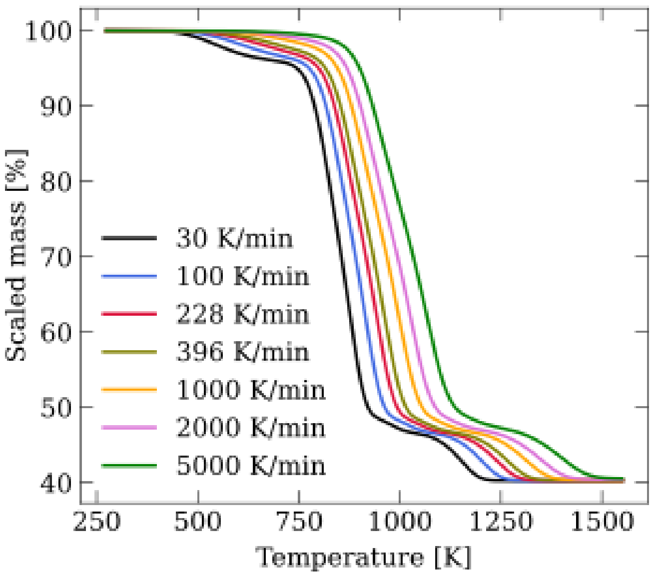

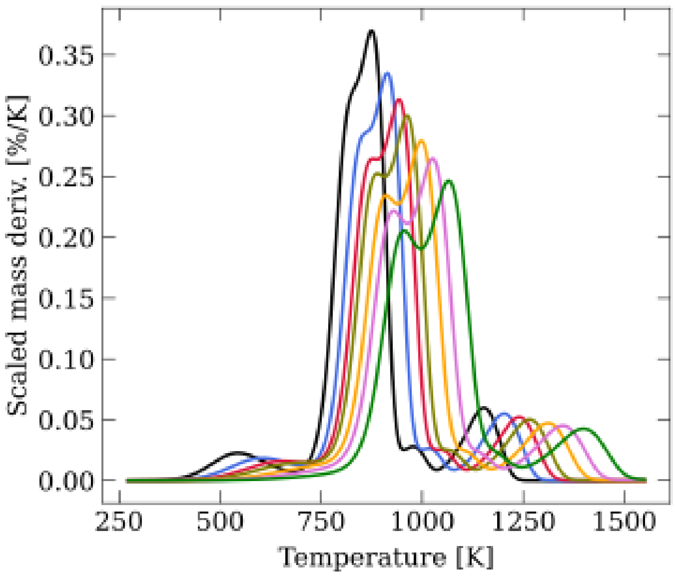

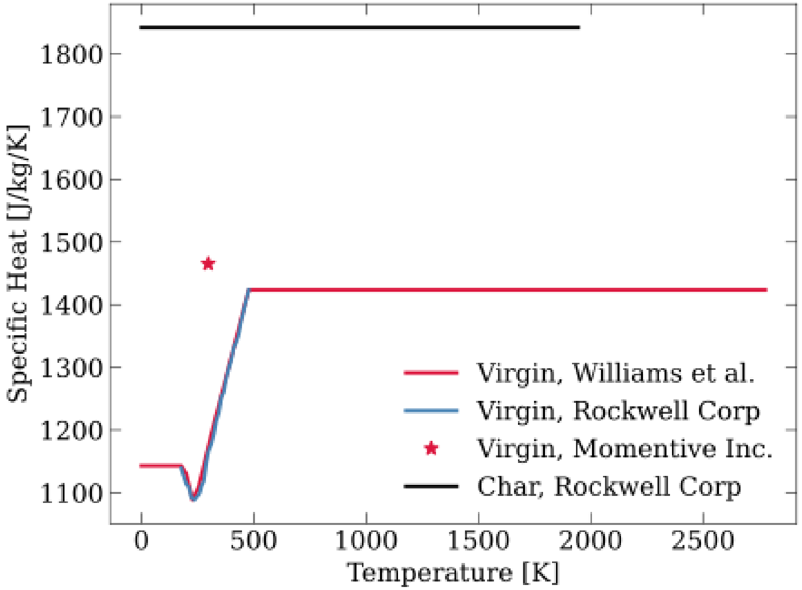

RTV Mechanical Properties Calibration

- Thermo-mechanical properties were only available till 500 °C and were calibrated for higher temperatures using the multi-pyrolysis approach
  - Calibrated using PATO coupled with Dakota based on 102 and 1946 °C/min data.

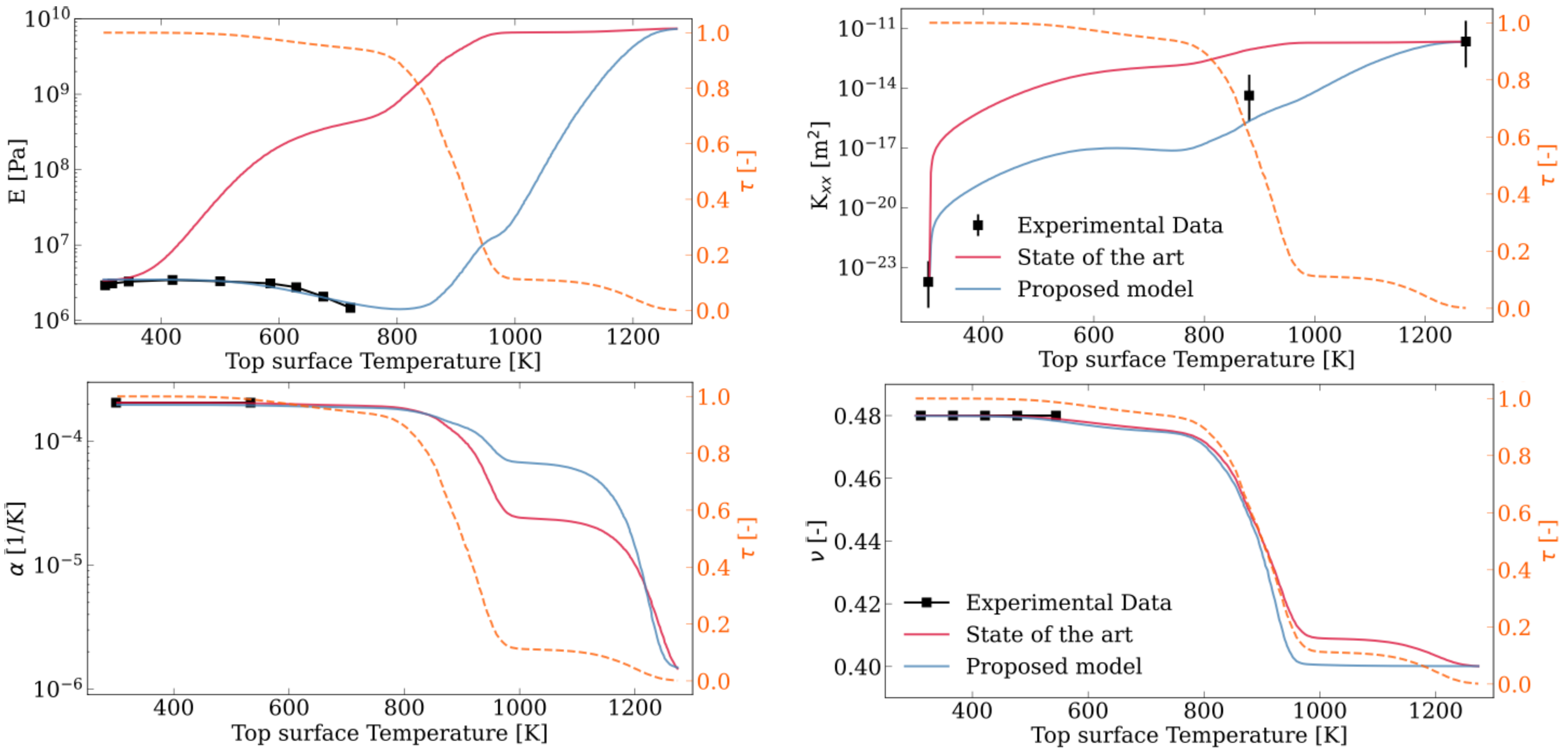

Thermo-poro-mechanics at 228 °C/min

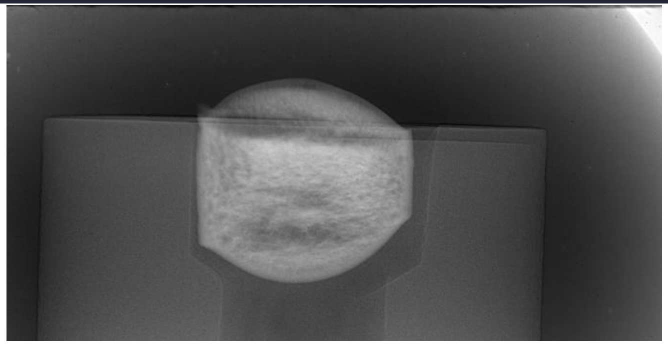

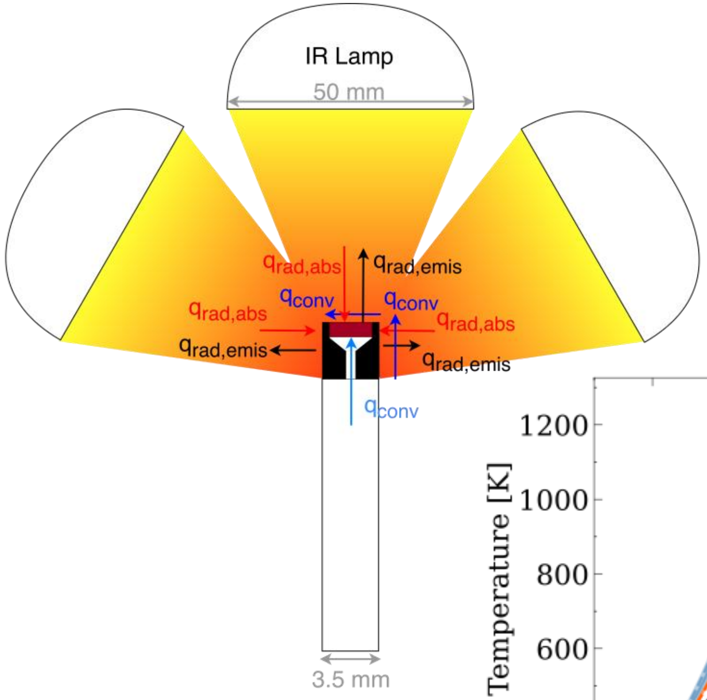

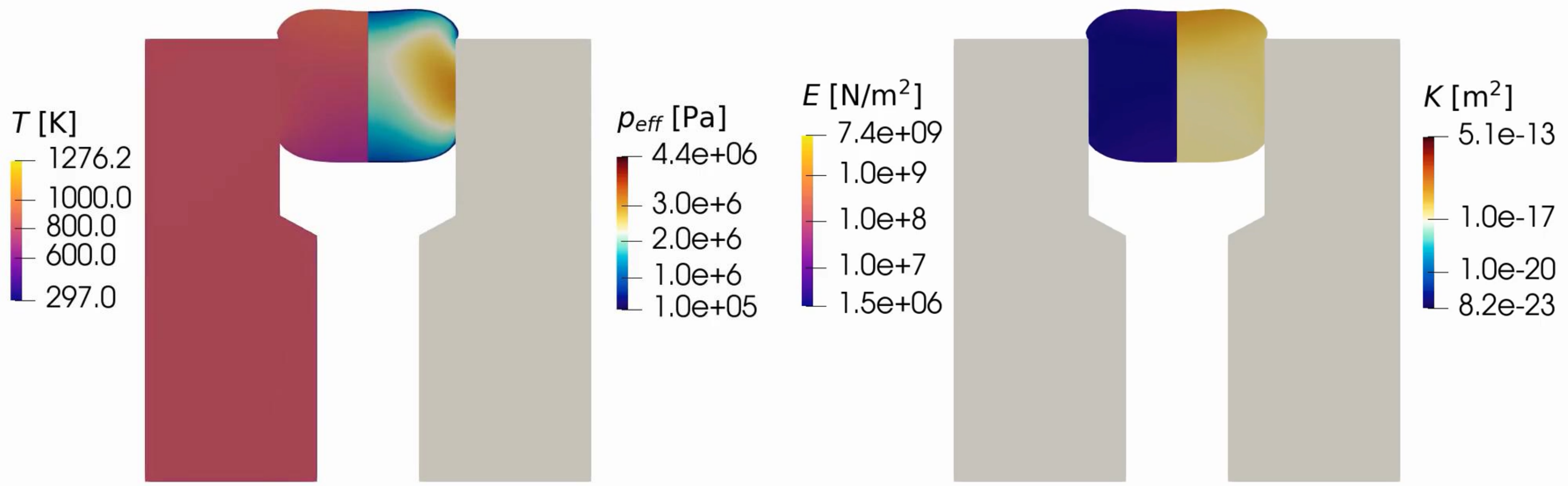

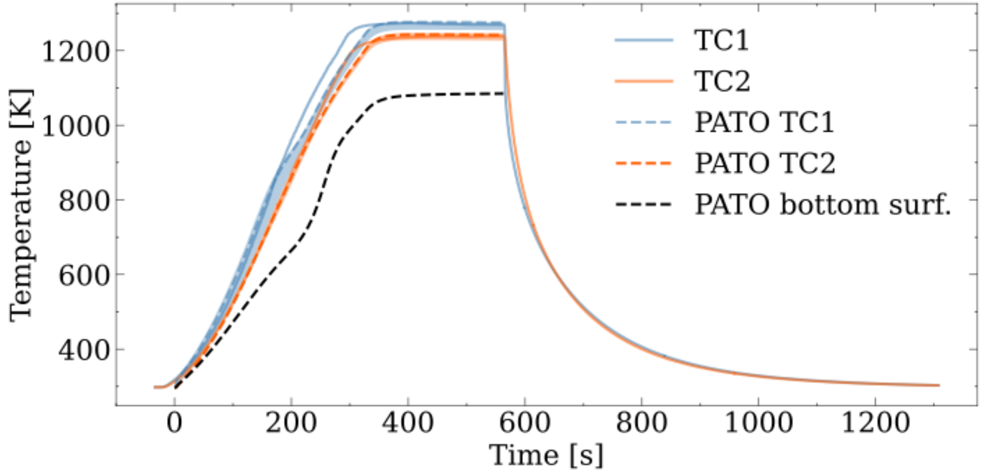

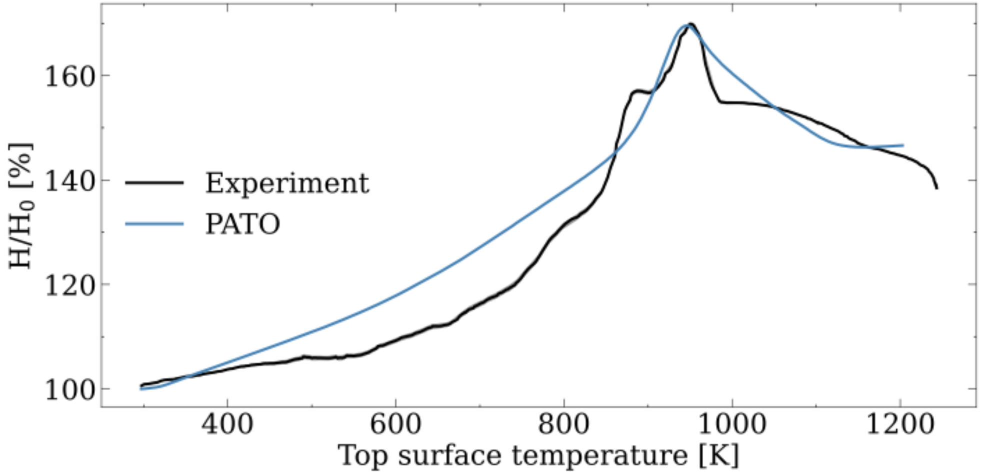

Simulations summary

Simulations at four heating rates showed good agreement:

- Thermo-poro-mechanics of closed- and open-pore pressure buildup and shrinkage was well-captured by simulations,
- Large variations in material properties are accounted for using multi-pyrolysis model,
- Further calibration of temperature profiles could improve results at higher heating rates.

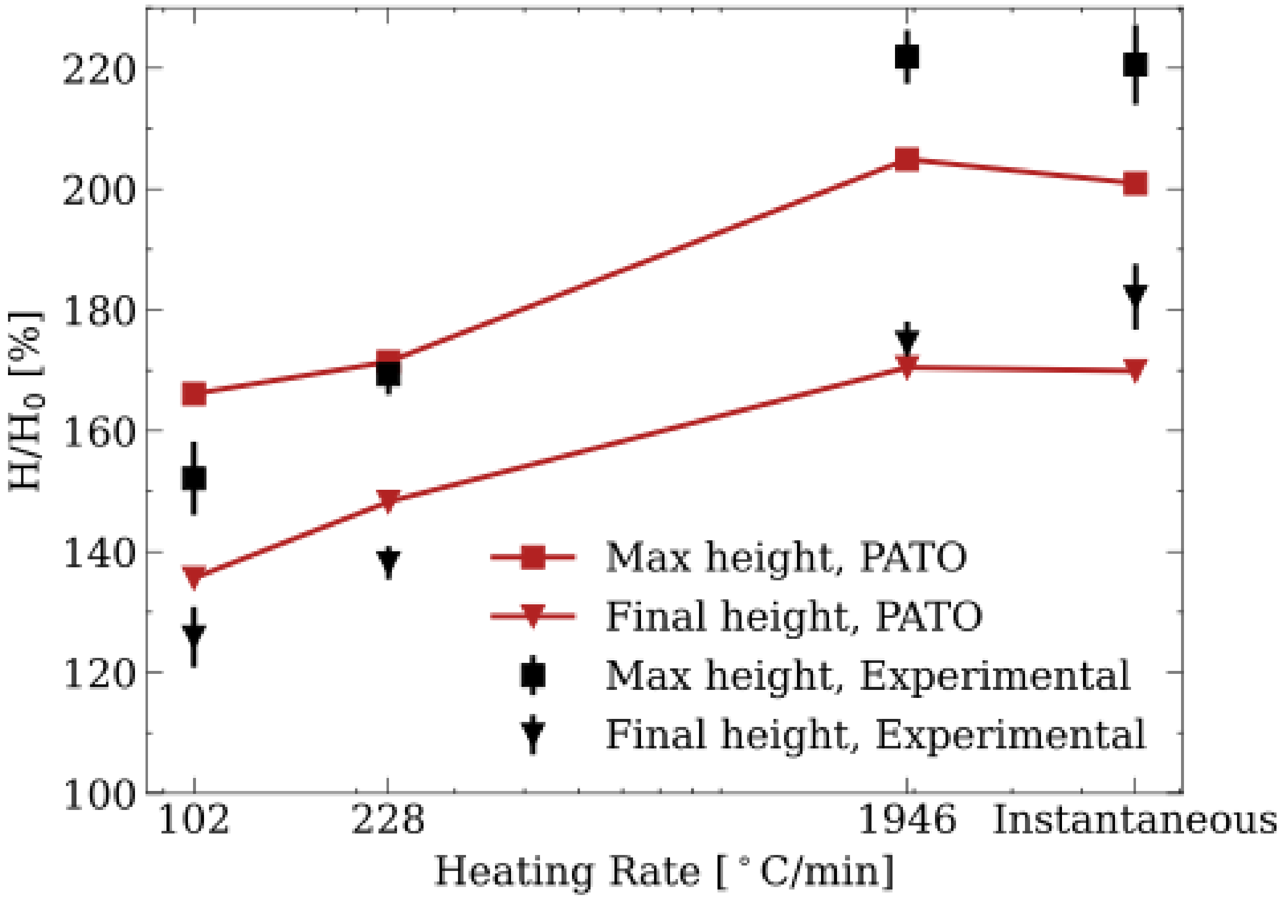

Conclusions

- Proposed a new intumescence mechanism for RTV based on experimental observations.
- Developed new Thermo-poro-mechanical capability to simulate intumescence:
  - Included closed porosity and closed-pore pressure buildup into PATO,
  - Introduced new *multi-pyrolysis* approach for capturing non-monotonic variations in material properties.
- Simulated RTV intumescence at high-heating rates:
  - Good agreement of thermal response with thermocouple measurements,
  - Mechanical response compared well with *in situ* radiography.

Future Work

1. Implementation of cracking, finite-rate gas-surface interactions and RTV wicking into porous materials,

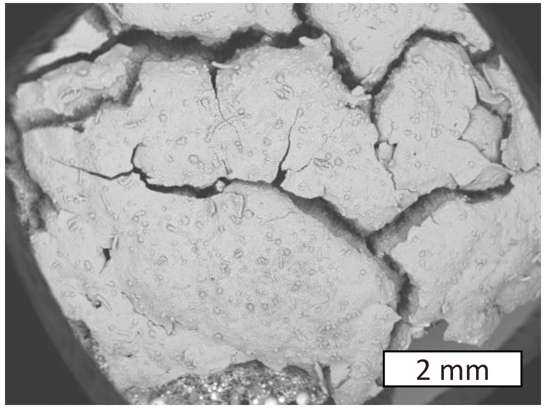

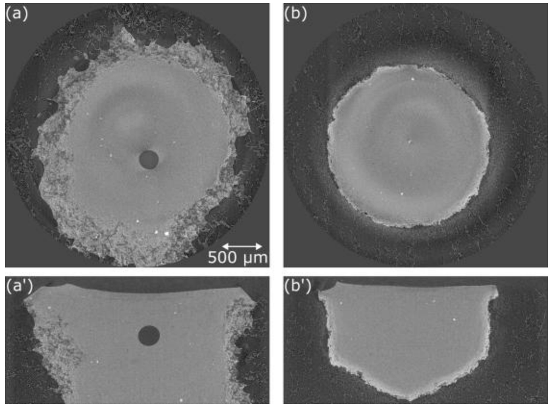

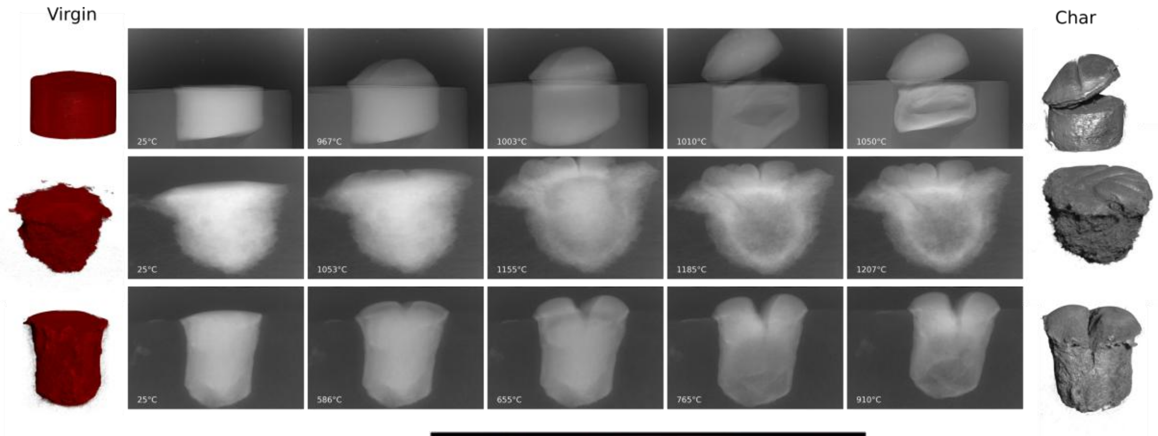

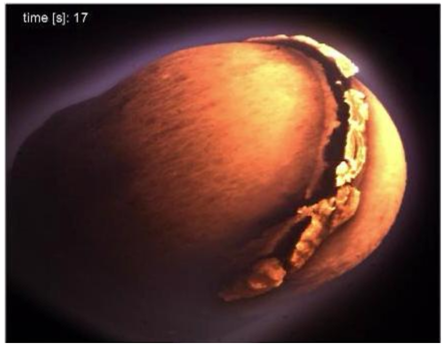

Future Work

1. Implementation of cracking, finite-rate gas-surface interactions and RTV wicking into porous materials,
2. Anchoring the multi-pyrolysis model to more material properties,

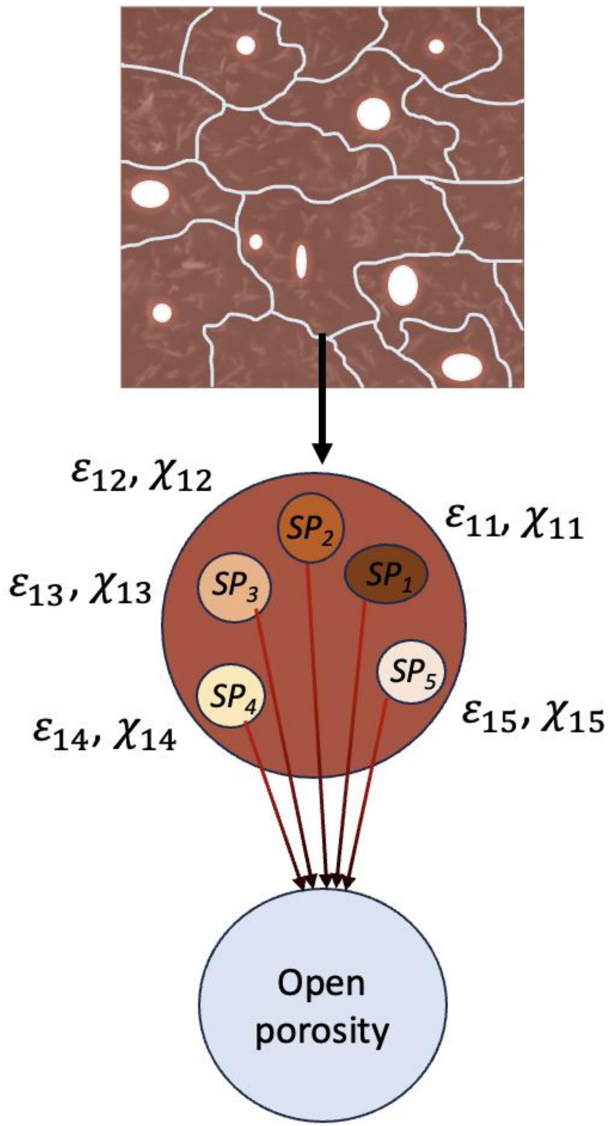

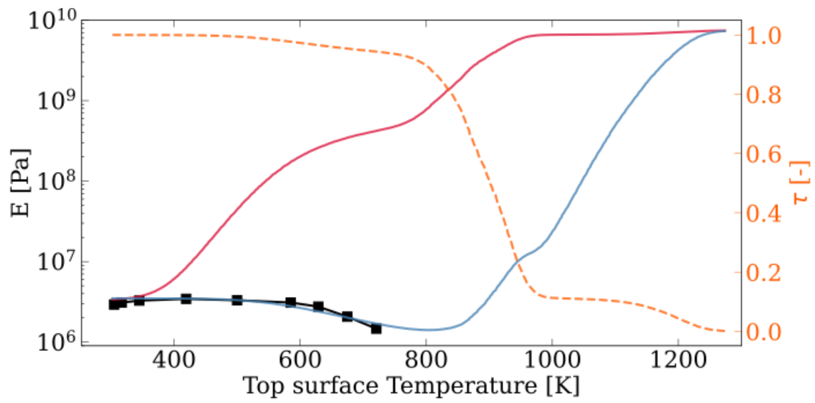

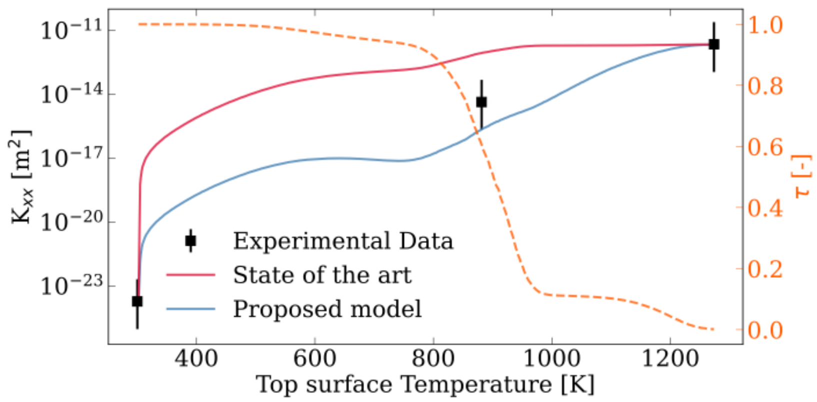

Future Work

1. Implementation of cracking, finite-rate gas-surface interactions and RTV wicking into porous materials,
2. Anchoring the multi-pyrolysis model to more material properties,
3. Simulation of Plasmatron X experiments,

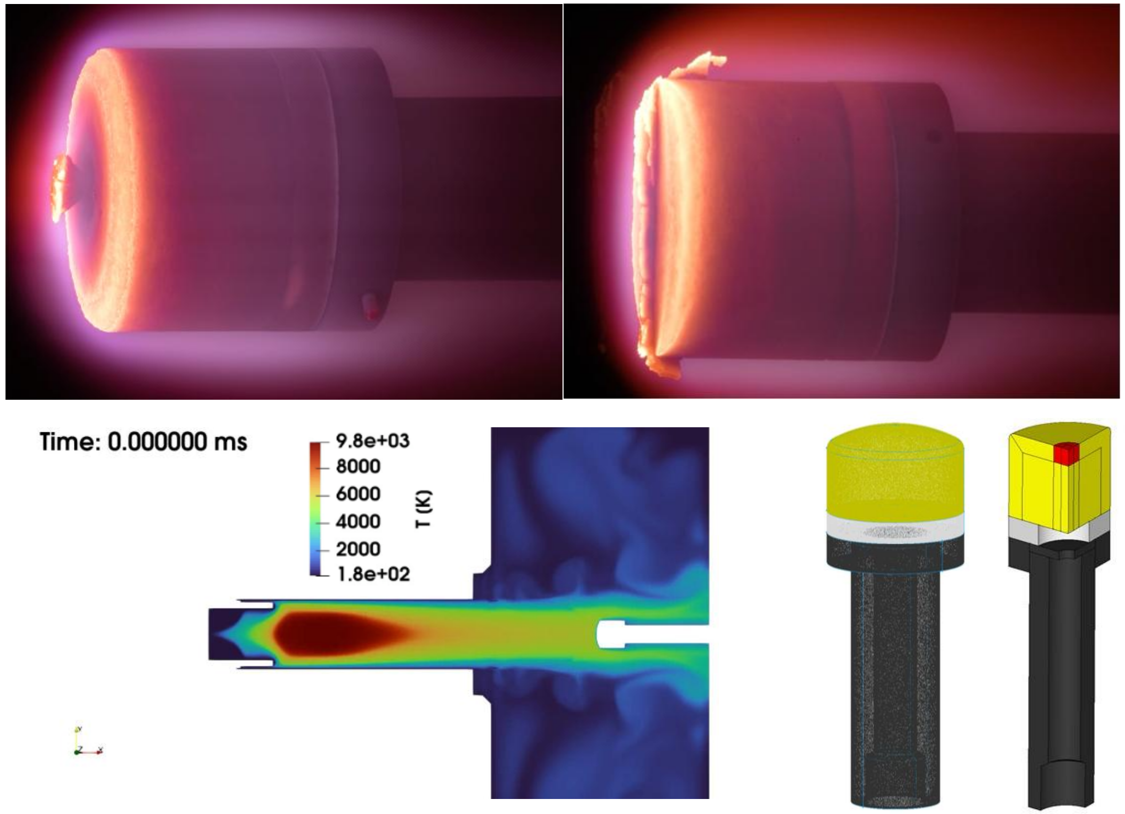

Flow field simulations of Plasatron X facility around an iso-*Q* sample *(Kumar et al.*[16-19]*)*.

Future Work

1. Implementation of cracking, finite-rate gas-surface interactions and RTV wicking into porous materials,
2. Anchoring the multi-pyrolysis model to more material properties,
3. Simulation of Plasmatron X experiments,
4. Simulation of tiled heat shields and mitigation strategies for fencing,

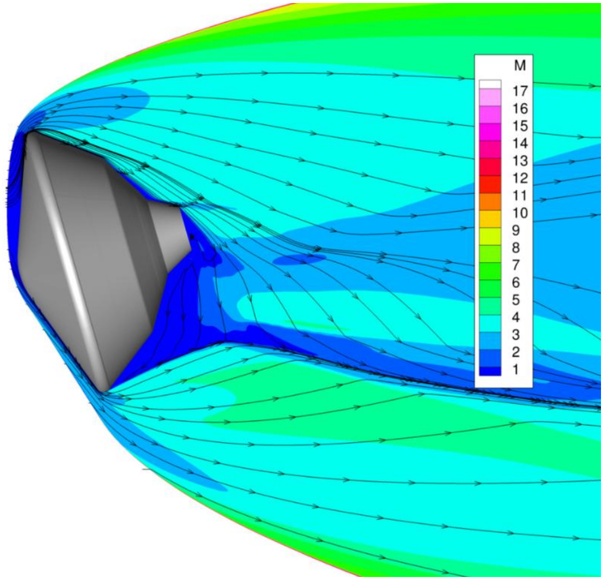

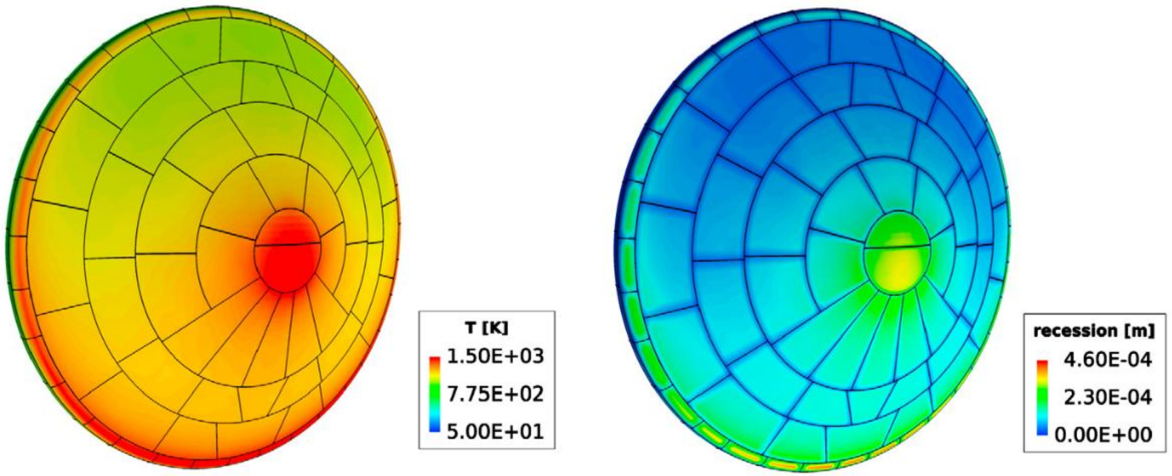

Mars Science Laboratory heatshield simulation in PATO (*Meurisse et al.* [15]).

Future Work

1. Implementation of cracking, finite-rate gas-surface interactions and RTV wicking into porous materials,
2. Anchoring the multi-pyrolysis model to more material properties,
3. Simulation of Plasmatron X experiments,
4. Simulation of tiled heat shields and mitigation strategies for fencing,
5. Rederivation of governing equations to include closed porosity and deformation of the domain.

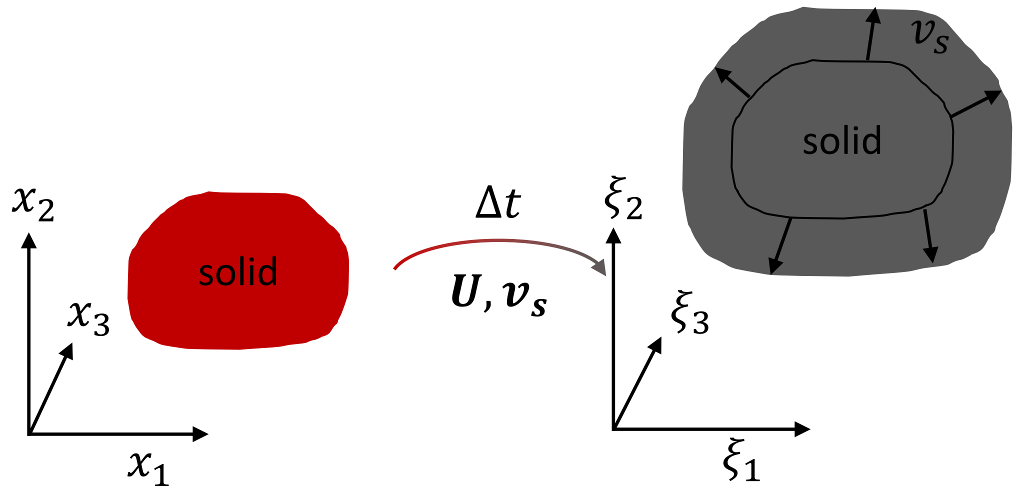

$$\partial_t \rho_s + \nabla \cdot (\rho_s \boldsymbol{v_{s,x_i}}) = 0$$

$$\partial_t \rho_s + \partial_{x_1}(\rho_s v_{s,x_1}) + \partial_{x_2}(\rho_s v_{s,x_2}) + \partial_{x_3}(\rho_s v_{s,x_3}) = 0$$

$$\Downarrow$$

$$\frac{\partial \rho_s}{\partial \tau} + \frac{\partial \xi_j}{\partial \tau}\frac{\partial \rho_s}{\partial \xi_j} + \frac{\partial \xi_j}{\partial x_i}\frac{\partial (\rho_s v_{x_i})}{\partial \xi_j} = 0$$

Acknowledgements

- This work was supported by
  - NASA NSTGRO
  - DOE SCGSR
  - NASA ACCESS and ESM projects

- Authors would like to thank:
  - ALS: Dilworth Parkinson, Collin Foster, Harold Barnard
  - Plasmatron X: Benjamin Ringel, Lorenzo Capponi
  - PATO: Jean Lachaud, Flora Lahouze, Blaine Vollmer

References

1. Mansour, Nagi N., et al. "Flow Mechanics in Ablative Thermal Protection Systems." *Annual Review of Fluid Mechanics* 56.1 (2024): 549-575.
2. Beck, Robin AS, et al. "Development of the mars science laboratory heatshield thermal protection system." *Journal of Spacecraft and Rockets* 51.4 (2014): 1139-1150.
3. Oruganti, Sreevishnu, et al. "Microstructure of pyrolyzing RTV silicone." *Polymer Degradation and Stability* 207 (2023): 110237.
4. Alunni, Antonella, and Tahir Gokcen. "Assessment of fencing on the Orion heatshield." *46th AIAA Thermophysics Conference*. 2016.
5. Tang, Chun, et al. "Numerical simulations of the boundary layer transition flight experiment." *48th AIAA Aerospace Sciences Meeting Including the New Horizons Forum and Aerospace Exposition*. 2010.
6. Mason, Michelle L., et al. "Experimental Aerothermodynamics: Recent NASA Langley Capabilities and Contributions." *AIAA AVIATION FORUM AND ASCEND 2024*. 2024.
7. Torres, Xavier M., et al. "Relationship between Filler Type, Thermomechanical Properties, and Aging of Rtv Silicone Foams." *Thermomechanical Properties, and Aging of Rtv Silicone Foams*.
8. Lang, Jack T., et al. "X-ray tomography applied to electrochemical devices and electrocatalysis." *Chemical Reviews* 123.16 (2023): 9880-9914.
9. Foster, Collin W., Sreevishnu Oruganti, and Francesco Panerai. "Real-time quantitative imaging of RTV silicone pyrolysis." *Polymer Degradation and Stability* 214 (2023): 110403.
10. Foster, Collin, Sreevishnu Oruganti, and Francesco Panerai. "In-situ imaging of RTV silicone pyrolysis." *AIAA AVIATION 2023 Forum*. 2023.
11. Capponi, Lorenzo, et al. "Aerothermal characterization of the Plasmatron X wind tunnel: heat flux, stagnation pressure and jet unsteadiness." *AIAA Scitech 2023 Forum*. 2023.
12. Oldham, Trey, et al. "Aerothermal characterization of the Plasmatron X wind tunnel: optical emission spectroscopy and jet temperature reconstruction. " *AIAA Scitech 2023 Forum*. 2023.
13. Lachaud, Jean, and Nagi N. Mansour. "Porous-material analysis toolbox based on OpenFOAM and applications." *Journal of Thermophysics and Heat Transfer* 28.2 (2014): 191-202.
14. Meurisse, Jeremie BE, et al. "Multidimensional material response simulations of a full-scale tiled ablative heatshield." *Aerospace Science and Technology* 76 (2018): 497-511.
15. Lahouze, Flora, et al. "Pyromechanics: A solid mechanics approach to deformation during pyrolysis." *Fuel* 390 (2025): 134557.
16. Munafò, Alessandro, et al. "Hegel: a high-fidelity flexible software for hypersonics and plasma simulations." *AIAA Scitech 2024 Forum*. 2024.
17. Munafò, A., et al. "A Multi-Physics Modeling Framework for Plasma Wind Tunnels."
18. Kumar, Sanjeev, et al. "From Coils to Surface Recession: Fully Coupled Simulation of Ablation in ICP Wind Tunnels." *arXiv preprint arXiv:2602.15500* (2026).
19. Oruganti, Sreevishnu, et al. "Modeling instrumented test articles for Plasmatron X aerothermal environment." *AIAA Aviation 2023 Forum*. 2023.

Thank you!

Any questions or comments?

Backup